



Selection of Histological Parameters for the Development of an Analytical Method for Discriminating Fresh and Frozen/Thawed Common Octopus (*Octopus vulgaris*) and Preventing Frauds along the Seafood Chain

L. Tinacci¹ · A. Armani¹ · G. Scardino¹ · A. Guidi¹ · D. Nucera² · V. Miragliotta¹ · F. Abramo¹

Received: 17 April 2020 / Accepted: 15 July 2020
© The Author(s) 2020

Abstract

This study aimed at selecting effective histological indicators of the freezing process, for the discrimination of fresh and frozen common octopus *Octopus vulgaris*. Histological indices of freezing process were selected in mantle and arm muscle and axial nerve tissues. Seven histological parameters were chosen: overall muscle tissue structural organization (a); gaping among muscle bundles (b); presence of optically empty spaces between and within muscle bundles (c); white spaces percentage between and within muscle bundles (d); overall nerve structural organization (e); presence of linear fissures and/or empty spaces within neuropil and axonal tract (f); presence of empty spaces within connective tissue matrix surrounding the nerve (g); empty space percentage within arm axial nerve region (h). The parameters were assessed on 150 mantle muscle sections (a, b, c, d), 150 arm muscle (b, c) and nervous (e, f, g, h) tissue sections belonging to 20 fresh exemplars further subdued to conventional freezing procedure at $-20\text{ }^{\circ}\text{C}$, 25 fresh curled exemplars, 25 exemplars industrially frozen at $-80\text{ }^{\circ}\text{C}$, and 20 thawed, curled, and individually quick frozen exemplars. Overall structural organization (a, e), gaping (b), and presence of optically empty spaces (c, f) confirmed significant morphological freezing indices in mantle and arm sections. In mantle, two d values ($d < 25\%$ and $25\% < d < 33\%$) were proposed as complementary thresholds to be applied in association with b and c indices for freezing discrimination. These parameters appear eligible to set a method for discriminating fresh/thawed octopus products to be applied both in official control and self-check activities.

Keywords Cephalopods · Fraudulent substitutions · Mantle · Arm · Freezing · Tumbling

Introduction

Cephalopods represent the third seafood category after fish and crustacean products consumed in Europe (EUMOFA 2018, 2019). Markets' interest toward cephalopods is due to their high worldwide biomass availability, high palatability, and nutritional value (Vieites et al. 2019; Mouritsen and Styrbæk 2018; Khan and Liu 2019). In addition, the growing

popularity of Japanese sushi and sashimi has helped to further boost demand for cephalopods (Armani et al. 2017; FAO 2018). However, due to the continuous increase of fishing pressure and recurring environmental catastrophes, medium- and long-term catch estimates have been severely reduced (FAO 2018). Consequently, the market price of all commercial cephalopod categories such as squid (Order Teuthida and Sepiolida), cuttlefish (Order Sepiida), and octopus (Order Octopodida) (Arkhipkin et al. 2015; FAO 2018) have been constantly increasing in the presence of still high and stable market demand (FAO 2019).

The natural tissue toughness of cephalopods due to the collagen structure may discourage product acceptability by the consumers (Gokoglu et al. 2017). In addition, their limited shelf life due to the early spoilage (Hurtado et al. 1999; Vaz-Pires and Barbosa 2004; Vaz-Pires and Seixas 2006; Lougovois et al. 2008; Sykes et al. 2009; Shalini et al. 2015) represents a significant hurdle to the marketability of

L. Tinacci and A. Armani contributed equally to this work.

✉ A. Armani
andrea.armani@unipi.it

¹ Department of Veterinary Sciences, University of Pisa, Viale delle Piagge 2, 56124 Pisa, Italy
² Department of Agriculture, Forest and Food Science, University of Turin, Largo Braccini 2, Grugliasco, Torino 10095, Italy

cephalopods in their natural/original form. Tissue toughness is generally resolved by tumbling in water solution, a mechanical beating in the presence of sodium chloride solution which leads to a partial collagen degradation and myofibrillar protein extraction (Katsanidis 2004; Gokoglu et al. 2017). As for extending product shelf life, several techniques are applied to control chemical–physical factors (temperature, water activity, acidity, redox potential) implicated in alteration phenomena (Leistner 2000; Ghaly et al. 2010). Super-chilling, chilling of pressurized products, and freezing are common preserving methods applied to extend product commercial life. Among them, freezing represents the elective method for cephalopod preservation (Hurtado et al. 2001; Ando et al. 2005; Gokoglu et al. 2018).

At present, other than unprocessed fresh products, cephalopod products available at purchase generally consist of the following types: eviscerated and tumbled fresh; frozen not eviscerated in bulk; eviscerated and subjected to double freezing with intermediate tumbling (authors' note). However, each of the preserving methods listed is known to potentially influence the organoleptic and technological quality of the product (Altissimi et al. 2017; Gokoglu et al. 2018). This aspect is particularly evident in defrost cephalopods in which drip formation occurring during thawing and the recovery of microbial spoilage mainly contribute to determine a sensible reduction in the product commercial value (Venugopal 2006). Also considering the occurrence of fraudulent substitution regularly recorded by the years (Uddin 2010; Upton 2015), the labeling mandatory information about the seafood preservation, as imposed by the European legislator (Regulation EU No. 1169/2011; Regulation EU No. 1379/2013), has an essential role to protect both fair trade policy and guarantee the consumer's informed choice and safety. The failure to declare it is therefore configured as a commercial fraud for food business operators' benefit to the detriment of the final consumer transparency with potential health concerns.

Such scenario imposes the development of analytical methods able to discriminate frozen and thawed products (Tinacci et al. 2018). Non-destructive and destructive methods based on the assessment of anatomical, physical, and chemical characteristics have been thoroughly investigated for fish products (Duflos et al. 2002; Uddin 2010; Bozzetta et al. 2012). In particular, the histological evaluation of microscopical tissue alterations induced by freezing process has been recently revived by virtue of its high accuracy, repeatability, and affordability for the discrimination of the freezing process on fish of different species (Bozzetta et al. 2012; Meistro et al. 2016; Tinacci et al. 2018; Strateva and Penchev 2019). In contrast, no similar studies are reported for cephalopods.

Common octopus (*Octopus vulgaris*) (FAO 2020) is one of the most exploited species for human consumption within the Order Octopodida entering the preparation of several traditional recipes especially in Spain, Portugal, and Italy (Mouritsen and Styrbaek 2018). As for the value of common octopus products on the Italian market, a significant gap between the average price of local fresh products (9–16 €/kg) and frozen products (4.50–9 €/kg) mostly imported from North African countries are reported in the last years (2017–2019) (ISMEA 2019, mercati, pesca & acquacoltura). Therefore, the present study is aimed at selecting effective histological indicators of the freezing process, for the discrimination of fresh and frozen *O. vulgaris*, considering its importance for the national market. A preliminary analysis of fresh octopus mantle and arm tissue sections was conducted for the selection of the analytical site and the evaluation of time-dependent tissue alterations occurring during the product's commercial shelf life. The selection of morphological and morphometric parameters was therefore carried out through the comparative analysis on histological sections obtained from raw fresh, tumbled fresh, frozen, and tumbled frozen products and verified through an appropriate statistical analysis. This study represents the first step for the settling up of a standardized procedure to combat illegal practices occurring in the seafood value chain.

Materials and Methods

Descriptive Analysis of Fresh Tissue Microanatomy and Evaluation of Time-Dependent Histological Modification

Sampling and Tissue Processing

Ten whole *O. vulgaris* exemplars (~300–400 g, caught within the previous 24 h) were collected at a local fish market and used to assess histological features in fresh tissue. To this purpose, two different body parts per exemplar were collected as described in Fig. 1. The exemplars were then preserved at around 0 °C, using eutectic plates in a fridge at 4 °C, and sampled again at 72, 144, and 192 h (3, 6, and 8 days, respectively). Day 8 was in fact chosen as the last day of product shelf life according to Barbosa and Vaz-Pires (2004). Samples from these exemplars were indicated as F72 mantle (M) or arm (A), F144.M or A, and F192.M or A (Table 1). The storage temperature was monitored daily with a digital probe thermometer (DT 90, TFA; Dotsmann GmbH & Co). All the tissue samples were promptly fixed and stored in a 10% buffered formalin solution (pH 7.4) for a minimum of 48 h. Then, prior to proceed with the further processing steps, the original samples of both mantle and arm were dissected in order to

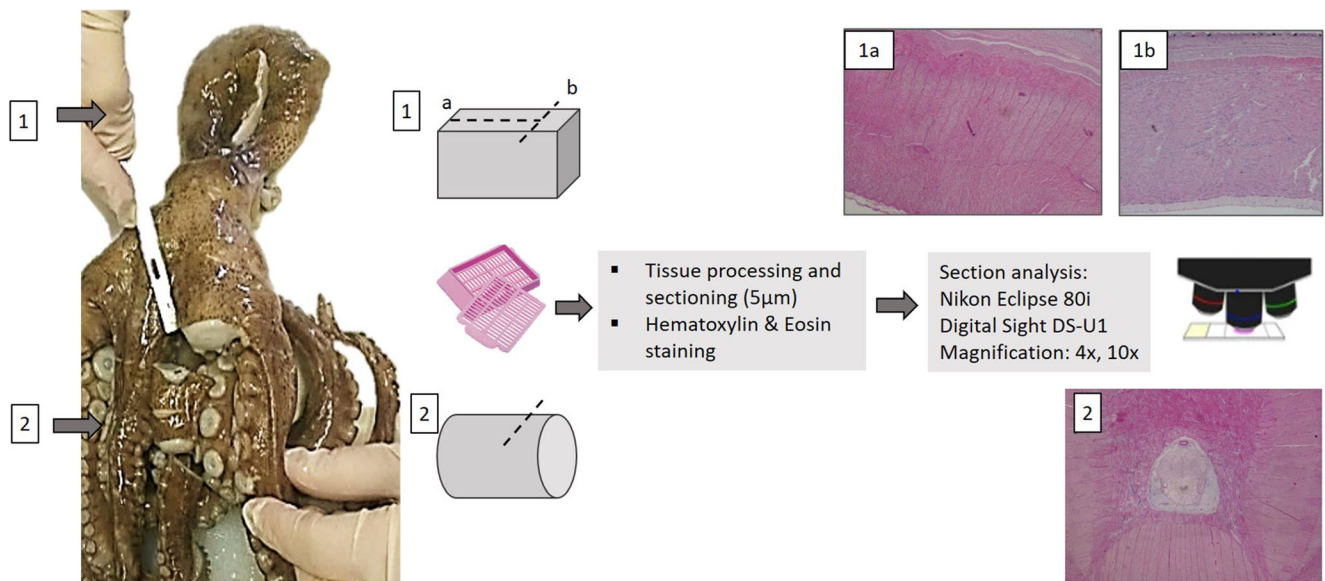


Fig. 1 Scheme highlighting the tissue processing (tissue sampling, section, and staining): (1) mantle sampling ((a) longitudinal section, (b) transversal section); (2) arm sampling and final histological section

obtain (a) 2 mantle blocks, 1 transversally and 1 longitudinally sectioned with respect to the mantle long axis, and (b) a transversal 2-mm-thick arm slice (Fig. 1). The two blocks belonging to mantle tissue and the arm slice for each exemplar were placed in separate histological cassettes and processed separately. Tissue processing of formalin-fixed samples was performed in a controlled automatic processor (VTP 300; BIOPTICA, Italy) and the sections finally stained with hematoxylin and eosin (H&E) as described in Tinacci et al. (2018).

Assessment of Fresh Tissue Histology and Histological Time-Dependent Tissue Modification on Fresh *O. vulgaris*

The obtained histological sections belonging to F24.M/A were observed under a light microscope (Nikon Eclipse 80i) connected to a Nikon digital camera (Digital Sight DS-U1) at $\times 4$ and $\times 10$ magnification and then photographed. A descriptive analysis of the *O. vulgaris* microanatomy was carried out to select the histological target sites within M and A sections.

Table 1 Total number of exemplars collected, and sections obtained and analyzed in the study

Tissue type	Number	Code	Treatment	Mantle section (M)	Arm section (A)	Sections total number
Fresh (24 h from capture)	10	F24.M/A	Collected and sampled	10	10	20
		F72.M/A	Stored at 0 °C, sampled at 72 h from capture	10	10	20
		F144.M/A	Stored at 0 °C, sampled at 144 h from capture	10	10	20
		F192.M/A	Stored at 0 °C, sampled at 192 h from capture	10	10	20
Fresh (24–48 h from capture)	20	F.M/A	Collected and sampled	20	20	40
		CF.M/A	Frozen in a conventional laboratory freezer at –20 °C for 15 days, thawed ON at controlled temperature (4 °C, 12 h)	20	20	40
Fresh tumbled	25	FT.M/A	Two beating cycles of 30 min in 3% NaCl saline solution according to the ordinary industrial plant processing procedure	25	25	50
Industrially frozen in bulk	25	IFB.M/A	Collected and sampled at industrial plant operating in seafood processing after an ON thawing in running water according to the plant ordinary procedure	25	25	50
Individually quick frozen	20	IQF.M/A	Double-frozen exemplars subdued to intermediate tumbling procedure, collected, and thawed ON at controlled temperature (4 °C, 12 h)	20	20	40
Total	100	–	–	150	150	300

ON overnight

The analysis aims at focusing on any eventual artifact produced during the processing. Five randomly selected fields belonging to F24, F72, F144, and F192.M and A sections were viewed at a $\times 10$ magnification to verify the presence of alterations such as the development of possible histological time-dependent modification during shelf life. All the areas occupied by time-dependent tissue alterations were recorded and described with NIS-Elements Br image analysis accompanying software (Nikon Instruments, Europe).

Histological Discrimination of Fresh and Frozen Common Octopus

Sampling

The following experimental groups of octopus exemplars, each characterized by different storing conditions and processing before tissue sampling, were obtained. (I) Twenty fresh whole exemplars of *O. vulgaris* (~300–400 g, caught within the previous 24 h), were collected at a local fish market. The exemplars were immediately sampled as described in the previous Section (Subsection [Sampling and Tissue Processing](#)) to obtain 40 tissue sections ($n = 20$ F.M and $n = 20$ F.A). (II) The same exemplars were frozen in a conventional laboratory freezer at $-20\text{ }^{\circ}\text{C}$ for 15 days and sampled again to obtain other 40 sections (CF.M, $N = 20$ and CF.A, $N = 20$). (III) Twenty-five additional fresh exemplars collected at 24 h from catch were subdued to manual cleaning and industrial curling process using a steel tumbler of 10 L capacity; at the end of the procedure, these fresh tumbled (FT) exemplars were transferred to the laboratory where a total of 50 sections (25 FT.M and 25 FT.A) were obtained. (IV) Further 25 wholes industrially

frozen in bulk (IFB) exemplars were collected from 10-kg *O. vulgaris* blocks after overnight thawing and used for obtaining 25 additional M (IFB.M) and 25 A (IFB.A) sections. (V) Finally, 40 tissue sections were obtained from 20 Individually Quick Frozen (IQF) curled *O. vulgaris* exemplars (IQF.M, $N = 20$; IQF.A, $N = 20$). Storing conditions and processing before tissue sampling of each different experimental groups of octopus exemplars are detailed in Table 1.

Selection of Morphological and Morphometric Parameters on M Sections

Sections belonging to the differently processed tissue samples (F, FT, CF, IFB, IQF) were preliminarily screened at $\times 4$ and $\times 10$ magnification. The central area of the longitudinal section crossed by a thin layer of connective fibers parallel to the longitudinal axis and including radial and circular muscle bundles was selected as analytical site for the mantle (Fig. 2). Three distinct morphological parameters were selected to be assessed: (a) overall tissue structural organization; (b) detachment or gapping among muscle fiber bundles; (c) presence of optically empty spaces between and within circular muscle bundles in form of round, oval, or saccular dilatation. Each parameter was associated with a qualitative score as detailed in Table 2. The percentage of white spaces between and within muscular bundles (parameter d) was selected to perform morphometry and then assessed on five consecutive field areas (1.14 mm^2). The function “Binary layer editing by threshold definition” available in the NIS-element software was used to select the areas occupied by stained tissue within each field by setting the threshold limits corresponding to the eosin-stained tissue. These areas, primarily represented by the

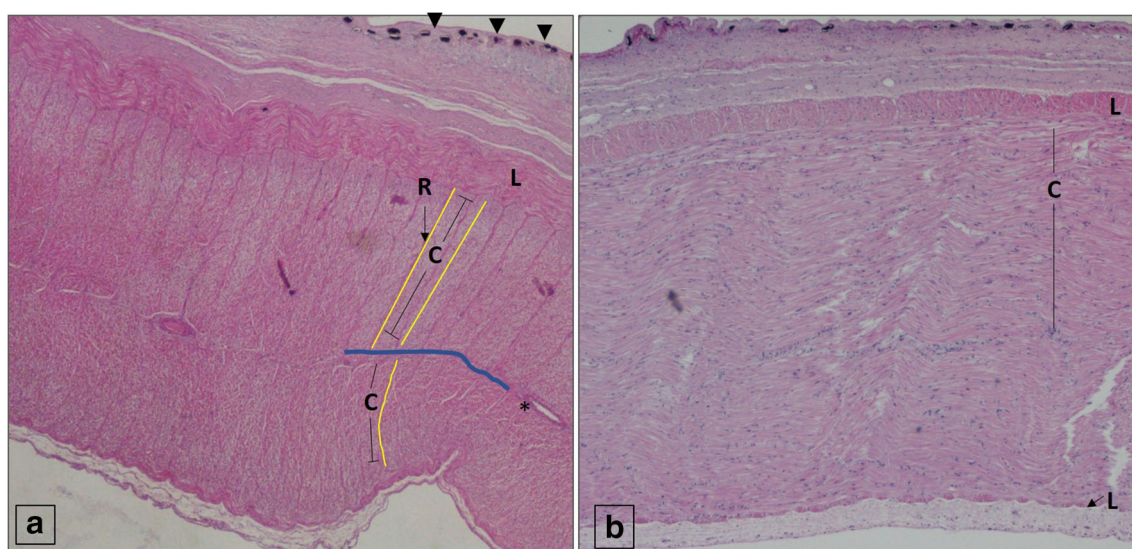


Fig. 2 Description of *O. vulgaris* fresh mantle. **a** Longitudinal section ($\times 2$): longitudinal muscle bundles (L), radial muscle fibers (R, orange lines), connective layer (blue line), vascular plexus (*). **b** Transverse section ($\times 2$): circular muscle bundles (C)

Table 2 Morphological and morphometrical parameters selected in the study with the relative scores

Body section	Parameter type	Description parameter	Score
Mantle	Muscle tissue	Morphological (a) Overall tissue structural organization (magnification $\times 4$)	0 = not altered, preserved (all the muscle bundles within the section clearly identifiable) 1 = altered
		(b) Detachment or gaping among muscle fiber bundles (magnification $\times 10$)	0 = not or minimally evident (gaping interesting less than the 10% of the observation field) 1 = mild/medium (interesting over 10% of the observation field area, with a clear separation between the fibers) 2 = marked (in presence of large longitudinal lacunar spaces surrounding muscle bundles)
		(c) Presence of optically empty spaces between and within circular muscle bundles in form of round oval or saccular dilatation (magnification $\times 10$)	0 = absent 1 = present
	Morphometric (d) Percentage of white spaces between and within muscular bundles (magnification $\times 10$)	Overall white space percentage/5 fields per section (field area = 1,139,837 μm^2)	
Arm	Muscle tissue	Morphological (b) Detachment or gaping among muscle fiber bundles (magnification $\times 10$)	0 = not or minimally evident 1 = mild/medium 2 = marked
		(c) Presence of optically empty spaces between and within circular muscle bundles in form of round oval or saccular dilatation (magnification $\times 10$)	0 = absent 1 = present
	Nervous tissue	Morphological (e) Overall nerve structural organization (magnification $\times 4$)	0 = not altered: not discernible alterations on nerve cord 1 = partially destructured: microanatomical modification of axonal tract and or cell lines or neuropil 2 = totally altered or destructured with a marked increase of tissue eosinophilia
		(f) Presence of linear fissures and/or round empty spaces or lacunae within the nervous tissue (neuropil and axonal tract) (magnification $\times 10$)	0 = absent 1 = present
		(g) Presence of oval-round empty spaces or lacunae interesting at least the 10% of the connective tissue surface surrounding the nerve	0 = absent 1 = present
		(h) empty spaces percentage within regions of interest (ROI) of axial nerve cord	White space percentage within each ROI

muscular fiber bundles and, to a lesser extent, by connective tissue, were measured to obtain the overall stained area. The overall white space area was then calculated by difference and then expressed as percentage on field area. The average of the percentages obtained on the five fields was assumed as representative value for each section. This parameter evaluated on fresh samples (F) at different shelf-life times served as control to exclude significant variations in the white space percentage during the commercial life.

Selection of morphological and morphometric parameters on A sections

The morphological analysis of the A section was conducted on two distinct tissue regions corresponding to the arm

musculature, and in particular to the central muscle layers (transverse, radial, longitudinal, and oblique bundles) surrounding the central nervous region, and the axial nerve cord region itself consisting of the axial nerve (axonal tract, neuronal cell bodies, and internal neuropil) and its surrounding connective tissue. For the evaluation of the central muscle layers around the nerve, the same morphological parameters (b) and (c) used to assess the mantle muscle fibers were applied (see Subsection [Selection of morphological and morphometrics parameters on M sections](#)). Both parameters were evaluated within a section area including longitudinal and radial bundles originating from the transverse musculature adjacent to the central loose connective tissue, in four quadrants (dorsal, ventral, lateral, and medial) (Fig. 3). For the morphological

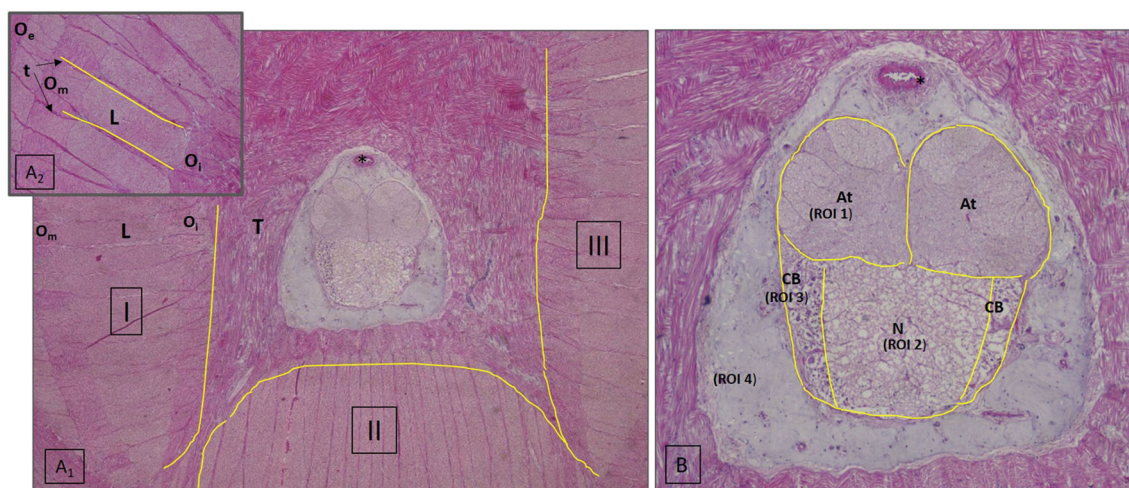


Fig. 3 (a1) *O. vulgaris* fresh arm section. T, transversal muscle fibers surrounding the axial nerve; O_i, internal oblique bundle muscles area located on the lateral sides of the transversal muscle region; L, longitudinal muscle area (limits of I-II-III quadrant highlighted by yellow lines); O_m, median oblique; O_e, external oblique musculature. (a2)

Particular ($\times 4$) of the longitudinal muscle area (L): trabeculae (t) radial course. (b) Axial nerve cord region surrounded by a thick connective tissue layer with loose irregular network of collagen fibers ($\times 4$): thick-walled artery (*), axonal tracts (At), neuropil (N), cell bodies (CB)

analysis of axial nerve cord region, three new parameters were introduced and evaluated at $\times 10$ magnification: (e) overall nerve structural organization; (f) presence of linear fissures and/or round empty spaces or lacunae within the nervous tissue (neuropil and axonal tract); (g) presence of oval-round empty spaces or lacunae interesting at least the 10% of the connective tissue surface surrounding the nerve (Table 2). A scoring system like that developed for the evaluation of the mantle was used (Table 2). For the morphometrical assessment of the empty space's percentage (parameter h), the axial nerve cord was preliminarily divided in four regions of interest (ROI), according to the tissue microanatomy, as follows: ROI 1 = axonal tracts, ROI 2 = the internal neuropil of the ganglion, ROI 3 = the neuronal cell bodies, and ROI 4 = the connective tissue surrounding the axial nerve cord. A threshold was manually defined to select the stained areas (occupied by the tissue) and not the white empty spaces within each ROI. The selected area was measured and expressed as a percentage of the respective traced ROI. The obtained results were a coefficient ranging between 0 and 1, inversely related to the presence of empty spaces (0 = entirely empty area (white); 1 = area entirely occupied by tissue (stained)).

Statistical Analysis

Parameters Assessed on the M Sections

The overall structural organization (parameter a) and the presence of optically empty spaces between and within circular muscle bundles (parameter c) were tested by the χ^2 test to compare frequency differences in samples within the five

groups (F, FT, CF, IFB, IQF). The score distribution (from 0 to 2) of the detachment or gapping among muscular fibers on the five groups was investigated using the Kruskal–Wallis test; if overall significance was observed, further differences among groups were assessed using the Mann–Whitney U test with $k - 1$ comparisons (with k representing the total number of examined groups). Finally, the percentage of white spaces was examined using the ANOVA test and subsequently a Student t test assuming equal variance within the sample populations. For all the analyses, significant results were those associated with $p < 0.05$.

Finally, differences among the percentage of white spaces calculated at different shelf life (F24.M, F72.M, F144.M, and F192.M) were assessed through the application of Student t test.

Parameters Assessed on the A Sections

The nerve structural organization and the presence of gapping between the surrounding longitudinal and radial fibers, both evaluated with a grading of 0.1.2, were analyzed by comparing the score distribution within the five groups (F, FT, CF, IFB, IQF) using the Kruskal–Wallis test, and differences between groups were assessed using Mann–Whitney U test with $k - 1$. The remaining qualitative parameters assessed with score 1 or 0 in the presence or absence of the modification under study (Table 2) were analyzed by comparing the frequency difference within the five groups with the χ^2 test. Finally, the percentage of empty spaces in the four pre-selected ROIs was analyzed using ANOVA and post hoc Bonferroni tests.

Results and Discussion

Sampling and Tissue Processing

All the tissue samples were successfully processed and a total of 300 sections (150 mantle longitudinal and 150 arm sections) were finally obtained and analyzed (Table 1).

Fresh Tissue Histology of Mantle and Arm Sections: Selection of the Analytical Site

Mantle Sections

Mantle's muscle appeared as a multi-layer tissue with the different muscle bundles oriented in different directions as in the description provided by Kier and Thompson (2003). In particular, proceeding from the outer to the visceral surface, three major areas were clearly identified and consisting of (1) an external area characterized by longitudinal muscles bundles running parallel to the longitudinal axis underneath the subcutaneous connective tissue; (2) a thick central area including radial muscle fibers departing from the longitudinal bundles and circular muscle fibers, where both of them crossed in the midline by a thin connective layer containing vascular and nervous plexuses; and (3) an inner area similar to the outer one, including an inner longitudinal muscle layer in contact with a thin connective layer (Fig. 2). The longitudinal section (Fig. 2a), in which all the muscle groups with different orientation were clearly visible, was selected as analytical target over the transverse section (Fig. 2b) in which the course of the radial fibers was not clearly discernible. Furthermore, the analysis of the outer part of the longitudinal section showed circular muscle bundles, particularly rich in mitochondria (SMR—superficial mitochondrial rich fibers) related to a predominantly aerobic metabolism, opposite to the primarily anaerobic metabolism characteristic of central mitochondria-poor fibers (CMR) observed in the inner part (Mommensen et al. 1981; Preuss et al. 1997; Bartol 2001; Kier and Thompson 2003). Although SMR exhibits a stable localization at the outer part of the longitudinal section, the development and the thickness of this peculiar muscle fiber bundles is subject to inter- and intraspecific variability (Mommensen et al. 1981), analogously to the distribution variability of aerobic (red) and anaerobic (white) fibers within fish muscle tissue (Tinacci et al. 2018). Thus, only the central part of the longitudinal section was selected as target of investigation and, particularly, the analysis focused on the central portion of the mantle core made up of circular and radial CMR-type muscle fibers, assuming a greater degree of intraspecific histological homogeneity (Bone et al. 1995).

Arm Sections

The transversal section considered in the study, produced by a perpendicular cut to the longitudinal axis of the arm, allowed the clear visualization of the central axial nerve cord region delimited by a thick connective tissue layer surrounding the central core and a peculiar three-dimensional arrangement of the surrounding arm musculature (Fig. 3). In brief, within arm musculature distinct areas consisting of muscle bundle fibers with different spatial orientation were identifiable and consisting of (1) a dense network of transversal muscle fibers extending approximately parallel to the sagittal plane and surrounding the central connective tissue, (2) two internal oblique bundle muscles located on the lateral sides of the transversal muscle region, (3) longitudinal muscle area subdivided into four quadrants departing from each of the transversal fibers network edge, and (4–5) median oblique and external oblique muscles consisting of two thick oblique bundles separated by a thin layer of longitudinal fibers located on the lateral sides of the arm section. Each quadrant of longitudinal muscle fibers was in direct contact with the inner bundle of oblique fibers, and both were crossed and divided into septa by thin bundles of transversal fibers with a radial course, described by Graziadei (1965). The arm microanatomy observed in this study is in accordance with the previous description of Kier and Thompson (2003), Kier and Stella (2007), Fossati et al. (2011), and Kier (2016). This natural microanatomical musculature partitioning was used to divide the histological section into standard target areas for the subsequent comparative analysis between fresh and frozen samples. Particularly, to standardize the site of study of the muscular component, the analysis was exclusively concentrated on the four quadrants of the longitudinal musculature. The axial nerve cord region consisted of a loose irregular network of collagen fibers and fibroblasts suspended within a relatively large amount of ground substance hosting a thick-walled artery located at the aboral surface of the axial nerve cord. The axial nerve cord was characterized by two dorsally located axonal tracts, layers of cell bodies belonging to a ganglia chain in the periphery, and the internal neuropil containing neuronal and glial cell processes were clearly identifiable. These microanatomic peculiarities were used as defined microanatomical targets for the setting of the morphological parameters to be specifically evaluated on the arm section (see Material and Methods: [Selection of morphological and morphometric parameters on A sections](#)). In particular, the localization of the main artery, in a dorsal position with respect to the nerve, was used as a landmark for the immediate section's orientation.

Four different ROI were identified within the nerve cord core as follows: ROI-1 including the two dorsally located axonal tracts; ROI-2 the internal neuropil; ROI-3 cell bodies; ROI-4 loose connective tissue (Fig. 3b).

Evaluation of Time-Dependent Histological Modification

The rapid postmortem onset of spoilage phenomena in cephalopods is primarily due to the proteolytic activity of endogenous enzymes directly affecting the muscular and connective tissue integrity (Hurtado et al. 1999). However, although sensorial schemes based on the analysis of organoleptic parameters, chemical and microbial indicators, and measurement of electrical tissue properties have been proposed to assess spoilage modification (Vaz-Pires and Barbosa 2004; Shalini et al. 2015), the spoilage-related histological alterations have never been investigated. On the contrary, evidence of spoilage-related histological changes is reported for both marine and freshwater fish species (George et al. 2016; Tinacci et al. 2018). In this light, a preliminary assessment of tissue spoilage occurring during the product shelf life was included in order to highlight possible histopathologic postmortem changes affecting the selection of morphological and morphometric parameters to be used for the differentiation of fresh and frozen products.

Mantle Sections

The assessment of fresh *O. vulgaris* at different shelf-life times showed mild structure changes and the tissue microanatomy was generally preserved up to 192 h of storage. Few degenerative alterations were highlighted affecting the circular muscle fibers in association with connective tissue alterations. In particular, the recorded alterations were represented by (1) increase of gaping between radial and circular bundles (Fig. 4a, b), (2) swelling of connective tissue surrounding small vessels and peripheral nerves and central connective layer (Fig. 4b, c), (3) local muscle bundle degeneration with increased fiber diameter (Fig. 4a), and (4) focal lytic areas (Fig. 4c, d). Myofiber degeneration was observed in F72.M, F144.M, and F192.M which presented few scattered swollen muscle fibers within circular muscle bundles. The affected myofibers presented a round-shaped section and a greater diameter with respect to the adjacent intact fibers (Fig. 4a). Finally, local or diffused lytic areas were mainly highlighted in the section belonging to F144.M and F192.M samples (Fig. 4c, d). The myofibril alterations observed were like those described on *Merluccius merluccius* samples preserved on ice

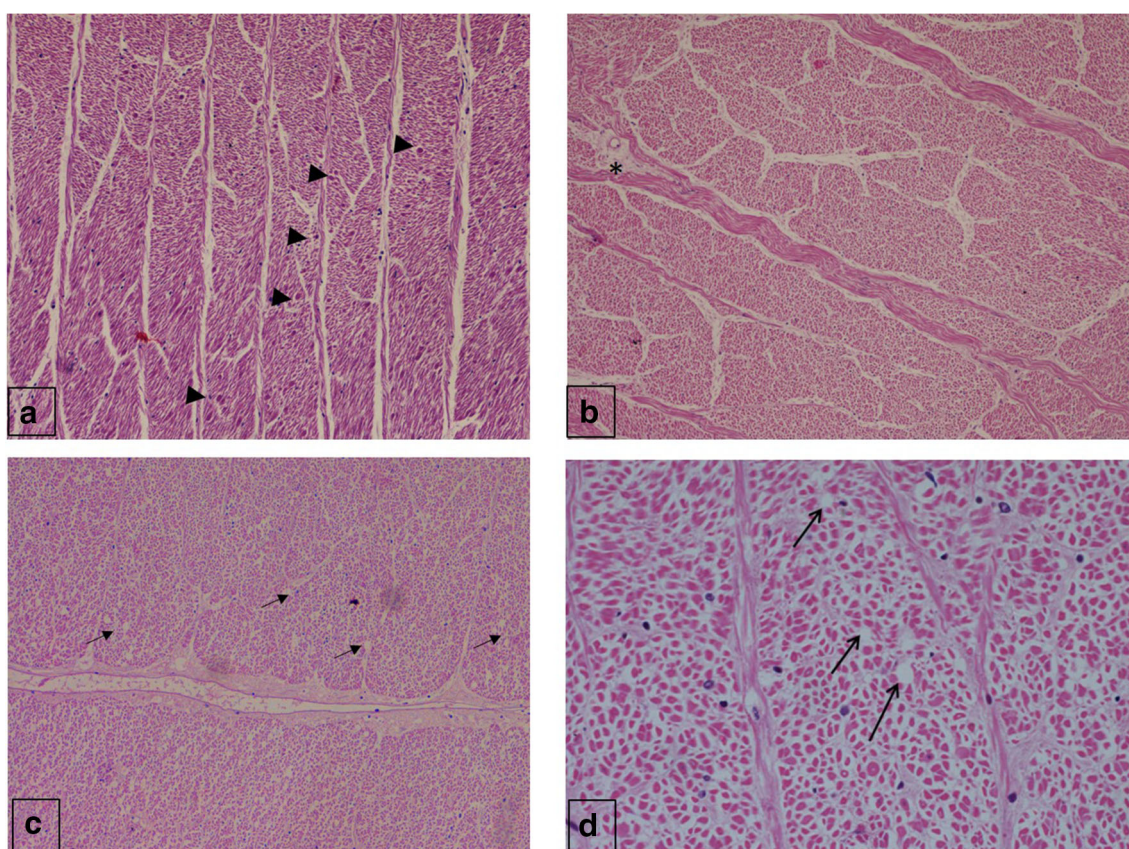


Fig. 4 Histology of *O. vulgaris* mantle and arm section at different shelf-life times. **(a)** F144.M ($\times 10$) mild gaping between radial and circular bundles, scattered swollen myofibers (black arrow heads); **(b)** F192.A ($\times 10$): mild muscle bundles gaping, local connective tissue swelling (*);

(c) F144.M ($\times 4$): small circumscribed lytic areas (black arrows), swelling of connective tissue central layer; **(d)** F192.A ($\times 20$) circumscribed lytic areas (black arrows)

for 72 and 120 h (Tinacci et al. 2018). Evident connective tissue swelling particularly pertaining to the central connective bundles layer was highlighted from 72 h post-harvesting (Fig. 4b).

Arm Sections

Myofibril alterations overlapping the patterns previously described were observed within the longitudinal fiber bundles of arm sections. Moreover, mild gaping between the trabeculae and the longitudinal fibers and the presence of focal areas of lysis were observed (Fig. 4c, d).

Comparative Analysis of Morphological and Morphometric Parameters of Fresh and Frozen M Sections

Parameter a: Overall Structural Organization

The analysis highlighted the maintenance of the micro-anatomical characteristics (score = 0, not altered, preserved) in all the fresh samples (F.M, FT.M) analyzed. Interestingly, the tumbling protocol experimentally applied in the study to fresh samples seemed not to determine any overall appreciable microstructural modifications. As regards the frozen samples, no alterations in the overall organization of CF.M were observed (Fig. 5a); on the contrary, remarkable alterations were observed in IFB.M group which shown uneven, from mildly altered (score = 0, 64%, Fig. 5b) to evidently altered (score = 1, 36%), microanatomical patterns. Finally, the maximum degree of tissue destructure was highlighted in IQF.M sections in which 55% of the samples showed evident alterations (Fig. 5c). The results obtained are apparently in contrast with the expected effects of the different types of freezing applied in the study. CF samples were in fact obtained through the application of a slow freezing protocol generally associated with the appearance of macro-crystallization in the extracellular site and subsequent tissue dehydration (Pham 2008). Contrariwise, the application of industrial rapid freezing generally results in ice nucleation within the intracellular areas creating a more structurally stable product and reducing osmotic induced tissue alterations (Petzold and Aguilera 2009). Thus, additional factors such as thawing procedure (in running water or at controlled temperature) must be considered in the worsening of the overall tissue microanatomy of IFB.M samples toward CF.M. Both factors, indeed, can contribute to the establishment of recrystallization phenomena with an increase in osmotic and mechanical stress on tissue microanatomy (Kolbe and Kramer 2007; Gokoglu and Yerlikaya 2015). Overall, significant differences emerged in the distribution of the structural patterns among the groups ($\chi^2 = 27.9$ $p < 0.05$) highlighting a significant freezing effect on the maintenance of the overall structural organization.

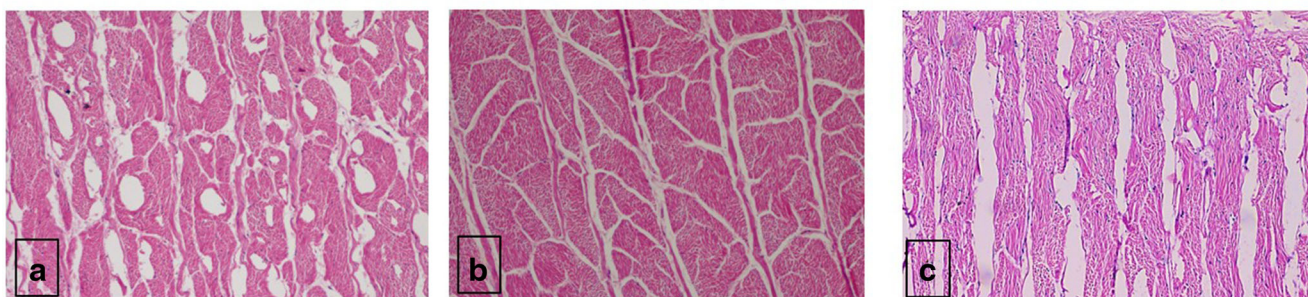
Parameter b: Gaping Among Muscle Fiber Bundles

The appearance of muscle gaping due to a damage of the collagen fibers caused by ice crystals within the tissue matrix has already been described in frozen fish muscle (Love and Robertson 1968; Love et al. 1969; Lavety 1991). In the present study, absent to minimal gap (score = 0) was recorded for all fresh samples (F.M and FT.M) while a medium (score = 1, Fig. 5a, b) to marked (score = 2, Fig. 5c) gaping was observed in all frozen sample categories. Table 3 shows the progressive increase in the gaping score and frequencies in the different types of frozen samples: the highest severity of gaping was found in IQF.M in which 90% of samples presented a marked gaping (score = 2). Kruskal–Wallis test showed high statistically significant differences ($H = 81.74$, $p < 0.05$) among the five groups. Further, Mann–Whitney test revealed a significant difference between the FM group and each of the freezing groups included in the study: CS.M ($z = -5.9408$ ($p < 0.05$)), IFB.M ($z = -6.14$ ($p < 0.05$)), and IQF.M ($z = -6.11$ ($p < 0.05$)).

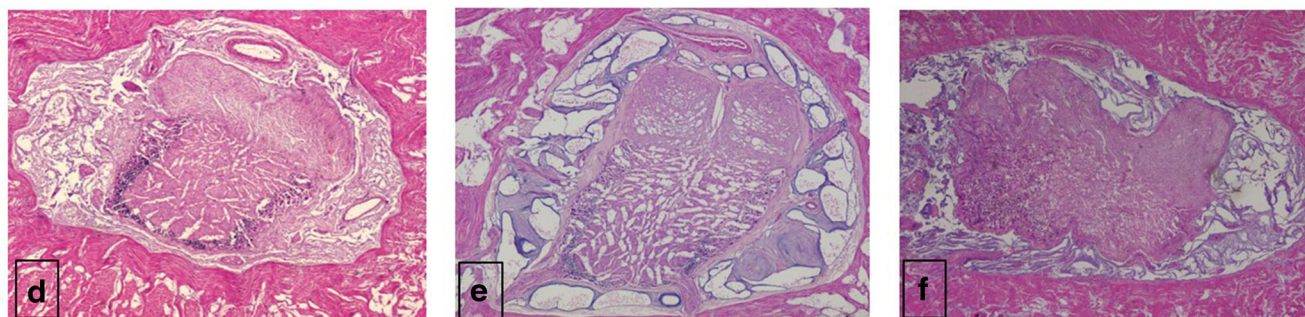
Parameter c: Presence of Optically Empty Spaces Between and Within Circular Muscle Bundles

The appearance of optically empty space has already been described in the literature among the modifications induced by freezing on the tissue of some cephalopod species (Ueng and Chow 1998). These changes are analogous to the alterations induced on fish tissue by the effects of water crystallization during the freezing and thawing phase (Pavlov et al. 2008; Bozzetta et al. 2012; Popelka et al. 2014; Tinacci et al. 2018; Strateva and Penchev 2019). In the present study, indeed, no optically empty spaces or sacciform gaps were highlighted in either F.M or FT.M samples (Table 3). In FT.M samples, local muscle bundles' degeneration patterns, similar to those previously described for fresh samples with different shelf life, were sporadically observed (Previous Section: [Evaluation of time-dependent Histological Modifications](#)). The appearance of these alterations was reconducted to the establishment of osmotic phenomena induced by 3% sodium chloride solution used for tumbling which can promote the passage of water toward the extracellular phase and further causing a contraction of the muscle fiber that appears to be markedly eosinophilic (Gokoglu et al. 2017). In contrast, optically empty spaces were observed with variable frequency in all frozen categories (Table 3). Empty space recorded in CS.M were generally represented by small size and rounded shape optically empty spaces, localized within the fiber bundles; saccular or oval connective tissue dilatations were mainly observed both optically empty and filled with lightly eosinophilic material in IFB samples; in IQF samples, inter-myofibrillar lacunae and round or oval spaces represented the prevailing alterations in all

Mantle section (10x)



Arm section axial nerve cord (4x)



Arm section muscle bundles (10x)

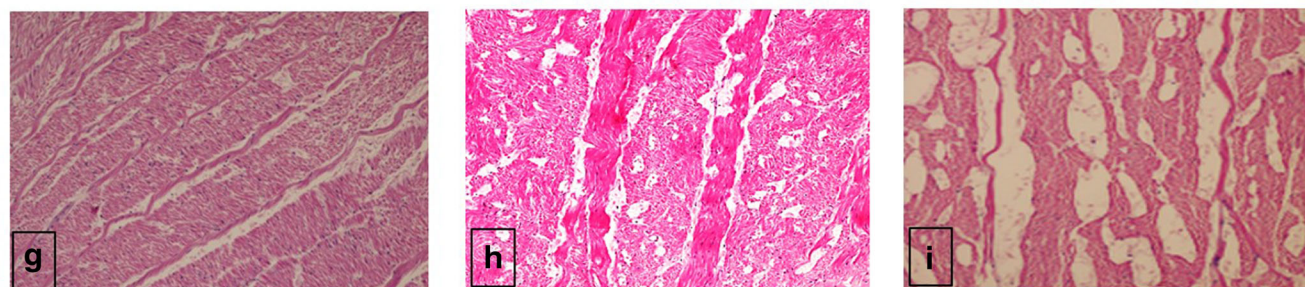


Fig. 5 *O. vulgaris* sections belonging to frozen tissue samples presenting different alterations. Mantle: (a) overall structure organization score = 0, muscle gaping score = 1, presence of round to oval optically empty spaces, score = 1; (b) overall structure organization score = 0, muscle gaping score = 1; (c) overall structure organization score = 1, muscle gaping score = 2, optically empty spaces score = 1 (sacciform gaps between and within circular muscle bundle). Arm: (d) overall nerve structural organization (score = 1), optically empty spaces located at the level of the neuropil and/or axonal tract (score = 1); (e) overall nerve structural organization (score = 1), optically empty spaces and cracks

located at the level of the neuropil and/or axonal tract (score = 1), presence of empty spaces or lacunae interesting at least the 10% of the connective tissue surface surrounding the nerve (score = 1); (f) nerve structural organization score = 2 (totally altered); (g) mild to medium muscle gaping (score = 1), presence of small optically empty spaces within longitudinal muscle bundles; (h) mild to medium muscle gaping (score = 1), presence of optically empty spaces within longitudinal muscle bundles and trabeculae (score = 1); (i) marked muscle gaping (score = 2) and optically empty spaces between and within longitudinal muscle bundles (score = 1)

the observation fields of each sample (Fig. 5b, c). χ^2 test applied on the data obtained from all the groups (F.M, FT.M, CF.M, IFB.M, and IQF.M) showed a significant effect of freezing in the appearance of empty spaces ($\chi^2 = 50.515$, $p < 0.05$). In order to further confirm the effect of freezing on the presence of vacuolar changes, the χ^2 test was applied for the comparison between the combined data of the frozen categories (CF.M; IFB.M; IQF.M) with the aggregate data of fresh samples (F.M; FZ.M) obtaining, also in this case, significantly different frequencies ($\chi^2 = 72.23$, $p < 0.05$).

Parameter d: White Space Percentage Between and Within Muscle Bundles

A progressive increase of the value was recorded from fresh tissue samples F.M (22.97%; minimum 15.31, maximum 31.19) and FT.M (22.53%; minimum 16.41, maximum 28.11) to CF.M (43.09%; minimum 32.71, maximum 57.90) and IFB.M (46.57%; minimum 39.10, maximum 57.88) and more importantly to IQF.M (59.69%; minimum 53.67, maximum 74.24) samples. The mean percentages calculated for each tissue category, investigated with ANOVA test,

Table 3 Results of the assessment of morphological and morphometric parameters on mantle histological sections of fresh (F.M), fresh tumbled (FT.M), conventionally frozen (CF.M), industrially frozen in bulk (IFB.M), and individual quick frozen (IQF.M)

Tissue processing category	(a) Overall tissue structural organization		(b) Detachment or gapping among muscle fiber bundles		(c) Presence of optically empty spaces between and within circular muscle bundles		(d) White space percentage between and within muscles bundles			
	0 = non-altered or minimally altered (< 10% of the observation field)	1 = altered	0 = absent or minimum observed in < 10% of the observation field	1 = mild or medium in > 10% of the observation field, with a clear separation between muscle bundles	0 = absent	1 = present	Mean %	Min %	Max %	95% CI
F.M (n = 20) (100%)	20	0	20 (100%)	0	0	0	22.97	15.87	31.19	2.01
FT.M (n = 25) (100%)	25	0	25 (100%)	0	0	0	22.61	16.41	28.11	1.28
CF.M (n = 20) (100%)	20	0	0	14 (70%)	6 (30%)	3 (15%)	42.05	32.71	57.90	3.53
IFB.M (n = 25) (64%)	16	9 (36%)	0	8 (32%)	17 (68%)	7 (28%)	45.77	39.10	57.89	2.55
IQF.M (n = 20) (45%)	9	11 (55%)	0	2 (10%)	18 (90%)	0	59.30	53.67	74.25	2.47

confirmed significant different across groups ($F = 187.10$, $p < 0.05$). The significance differences were further confirmed by Student *t* test results applied for the pair comparison of F.M vs. CS.M ($p < 0.05$), CS.M vs. IFB.M ($p < 0.05$) and IFB.M vs. IQF.M ($p < 0.05$). On the contrary, the same test used for the comparison between F.M and FT.M did not show a significant difference between the two groups ($p > 0.05$). The values obtained were consistent with the results described previously for the qualitative parameters. The expected value of the percentage of white measured in histological sections belonging to frozen tissue appeared increased compared with the fresh and fresh tumbled tissue plausibly due to the presence of gapping and optically empty spaces directly correlated to the phenomenon of crystallization and thawing procedure of the product (See SubSections parameter b and c). In fact, the assessment of the same parameter on F24.M, F.72.M, F.144.M, and F.172.M only showed an apparent percentage increase as follows: F.24.M (mean 23.98%; minimum 21.56, maximum 26.60), F.72.M (mean 25.00% in a range of 22.53–26.72), F.144 (mean 24.17%; minimum 22.21, maximum 27.48), and F.192.M (26.62%; minimum 23.79, maximum 28.40). In this respect, myofiber detachment or gapping due to endogenous enzymes proteolysis has been thoroughly investigated as one of the principal factors inducing breaking strength and softening of fish muscular tissue during chilled storage (Shigemura et al. 2003; Bahuaud et al. 2008; Roy et al. 2012; Sharifian et al. 2014). Nevertheless, the application of Student *t* test showed no significant differences among the percentages recorded within the sampling groups included in the study with the exception of F192.M, the percentage of which was significantly higher ($p < 0.05$) than each of the three previous shelf-life sampling groups (F24.M, F72.M, F144.M).

Comparative Analysis of Morphological and Morphometric Parameters of Fresh and Frozen A Sections

Parameters b (Gapping) and c (Presence of Optically Empty Spaces) Evaluated Between and Within Four Quadrants of the Central Muscle Layers Around the Nerve

All the samples belonging to fresh categories (F.A, FT.A) presented gapping = 0 except for a fresh sample in which a moderate gap was observed between the fibers with an extension greater than 10% in three out of four observation quadrants (gapping = 1) (Table 4). Within the frozen categories, a less evident gapping increase was observed compared with the data collected on the mantle. Indeed, an absent or minimum gapping (score = 0) was observed in 10% of CF.A, 10% of IQF.A, and 20% of IFB.A (Table 4) while a high frequency of mild gapping (score = 1) was generally highlighted in IQF.A (60%) sections (Fig. 5g), in contrast with the results obtained

Table 4 Results of the assessment of morphological parameters on arm histological sections of fresh (F.A), fresh tumbled (FT.A), conventionally frozen (CF.A), industrially frozen in bulk (IFB.A), and individual quick frozen (IQF.A)

Tissue processing category	(b) Muscle bundle gaping score	(c) Presence of optically empty spaces between and within circular muscle bundles	(e) Overall nerve structural organization	(f) Presence of linear fissures and/or round empty spaces or lacunae within the nerve tissue (neuropil and axonal tract)	(g) Presence of oval round empty spaces or lacunae within the connective tissue surrounding the nerve
	0 = absent or minimum observed in < 10% of observation field	1 = mild or medium separation between muscle bundles	0 = not altered	1 = present	1 = present
	1 = mild or medium in > 10% of the observation field, with a clear large longitudinal lacunar spaces surrounding muscle bundles	2 = marked, presence of large longitudinal lacunar spaces surrounding muscle bundles	1 = partially altered	2 = evident alteration	0 = absent
F.A (n = 20)	19 (95%)	1 (5%)	20 (100%)	0	20 (100%)
FT.A (n = 25)	25 (100%)	0	25 (100%)	0	23 (84%)
CF.A (n = 20)	2 (10%)	16 (80%)	19 (95%)	1 (5%)	2 (10%)
IFB.A (n = 25)	5 (20%)	5 (20%)	17 (68%)	8 (32%)	4 (16%)
IQF.A (n = 20)	2 (10%)	12 (60%)	18 (90%)	2 (10%)	0
					3 (15%)
					17 (85%)
					5 (25%)
					9 (36%)
					16 (64%)
					15 (75%)
					5 (25%)

on the mantle (Previous section, subsection [parameter b](#), Table 3). The reduced effect of freezing on the organization of the tissue could be relatable to the structural peculiarities of the arm's microanatomy described by Fossati et al. (2011) which might contribute to prevent alterations. In fact, other than a more complex arrangement of the musculature, the tissue is supported by a strong connective tissue net offering a stable anchor point for the muscle bundle departing in the centrifugal direction (Kier and Stella 2007; Fossati et al. 2011). Nonetheless, the statistical analysis performed with Kruskal–Wallis followed by Mann–Whitney test for the comparison in pairs of the 0–2 score frequencies recorded between the categories of fresh and frozen products confirmed significant differences in the score frequencies among all groups ($H = 80.03, p < 0.05$) and between the fresh category and each type of frozen product, Mann–Whitney: F.A versus CF.A, $z = -4.62, p < 0.05$; F.A versus IFB.A, $z = 4.44, p < 0.05$; F.A versus IQF.A, $z = -4.66, p < 0.05$) and between grouped frequencies of fresh versus frozen categories (F.A + FT.A versus CF.A + IFB.A + IQF.A, $z = 7.52, p < 0.05$). Regarding parameter c, similarly to the patterns highlighted on the muscular portion of the mantle, optically empty spaces were never observed in fresh tissue sections (F.A, FT.A). In contrast, optically empty spaces were observed in all frozen categories (CF.A; IFB.A, IQF.A) with higher frequency rates than those shown on mantle sections (Table 4, Fig. 5h, i). χ^2 test applied highlighted significant differences among fresh and frozen groups ($\chi^2 = 83.72, p < 0.05$).

Parameter e: Overall Nerve Structural Organization

The analysis confirmed the absence of alterations (score = 0) in the different areas of the axial nerve in all fresh samples (F.A and FT.A). On the contrary, in all frozen samples, microanatomical alterations of one or more structural components of the nerve (axonal tract, neuropil, ganglia, and cell bodies) were highlighted with a partial (score = 1, Fig. 5d, e) to complete alteration of the overall tissue structure (score = 2, Fig. 5f) (Table 4). Kruskal–Wallis test confirmed significant differences between the groups ($H = 80.083, p < 0.05$). Mann–Whitney test was subsequently applied for the comparison in pairs between F.A and each of the frozen categories, and a further comparison test between the aggregated data of the results obtained on the fresh (F.A, FT.A) and frozen categories (CF.A, IFB.A, IQF.A) revealed significant differences for each of the proposed comparisons (F.A vs. CF.A, $z = -5.39, p < 0.05$; F.A vs. IFB.A, $z = 5.69, p < 0.05$; F.A vs. IQF.A, $z = -5.39, p < 0.05$; F.A + FT.A vs. CF.A + IFB.A + IQF.A, $z = -8.88, p < 0.05$). The total absence of similar alterations in both fresh categories (F.A, FT.A) contributes to relate the overall microscopical nerve structural changes to the direct effect of osmotic phenomena and mechanical stress following the water crystallization phase during freezing and or

recrystallization during the tissue thawing or temporary cold chain interruptions (Kiani and Sun 2011).

Parameter f: Presence of Linear Fissures and/or Round Empty Spaces or Lacunae Within the Nervous Tissue (Neuropil and Axonal Tract)

No alterations were observed on the sections obtained from both fresh categories, with the exception of two FT.A in which cracks were observed inside the axonal tract of the nerve in the absence, however, of axon fiber degeneration. Contrariwise, a high frequency of one or both modifications was found in the samples belonging to the three frozen categories (Fig. 5d–f). In particular, within the IQF.A category, all the samples (100%) had optically empty spaces located at the level of the neuropil and/or axonal tract (Fig. 5e) not always accompanied by cracks. The significant effect of freezing toward the appearance of one of both alterations was further confirmed by χ^2

Table 5 Results of the assessment of the empty space percentage calculated in the four regions of interest (parameter h) (ROI 1 to ROI 4) in all the tissue sections belonging to the 5 different processing categories included in the study

Tissue processing category	%	ROI 1	ROI 2	ROI 3	ROI 4
F.A	Mean	16.86	29.7	30.28	17.12
	SD	9.03	14.35	9.98	12.97
	Max	37.3	62.8	13.4	1.8
	Min	7.6	7.9	45.7	52.9
	95% CI	4.23	6.71	4.67	6.07
FT.A	Mean	14.11	20.39	21.57	21.44
	SD	7.70	13.97	9.15	13.83
	Max	29.5	47.6	39.2	43.7
	Min	1.6	1.4	3.8	0.4
	95% CI	3.18	5.77	3.77	5.71
CF.A	Mean	8.4	14.56	11.5	27.97
	SD	4.42	6.62	6.18	14.04
	Max	17.4	4.7	24.7	50.7
	Min	1.7	28.1	2.5	1.3
	95% CI	2.07	3.10	2.89	6.57
IFB.A	Mean	15.98	17.22	12.95	38.04
	SD	13.86	13.26	10.76	18.32
	Max	44	47.7	42.2	79.3
	Min	1.8	1.3	0.9	16.5
	95% CI	6.48	6.21	5.03	8.57
IQF.A	Mean	15.13	24.84	16.65	32.97
	SD	11.70	13.99	10.67	16.54
	Max	40.4	53.7	41.9	71.9
	Min	2.2	3.1	2.4	5.6
	95% CI	5.47	6.54	4.99	7.74

test applied on the data obtained from all the groups ($\chi^2 = 67.32$, $p < 0.05$).

Parameter g: Presence of Oval-Round Empty Spaces or Lacunae Within the Connective Tissue Surrounding the Nerve

Alterations of the connective tissue matrix and presence of coalescent empty spaces or lacunae were found in all the tissue categories (Table 4). Despite the significantly different frequency between fresh and frozen products ($\chi^2 = 22.92$, $p < 0.05$), the presence of empty spaces within the connective tissue was observed in a not negligible percentage of both F.A (15%) and FT.A (64%) samples. The repetition of the χ^2 test with the inclusion of only the FT.A category together with all the categories relating to frozen products highlighted the loss of significance of the difference in the frequencies recorded for the parameter ($\chi^2 = 3.8012$, $p = 0.28$).

Parameter h: Assessment of the Empty Space Percentage within the Axial Nerve Cord ROI

Table 5 shows the results of the evaluation of the empty space percentage calculated in ROI1 to 4 in all the tissue sections (F.A, FT.A, CF.A, IFB.A, IQF.A). The same data expressed in graphical form are shown in Fig. 6. The ANOVA test

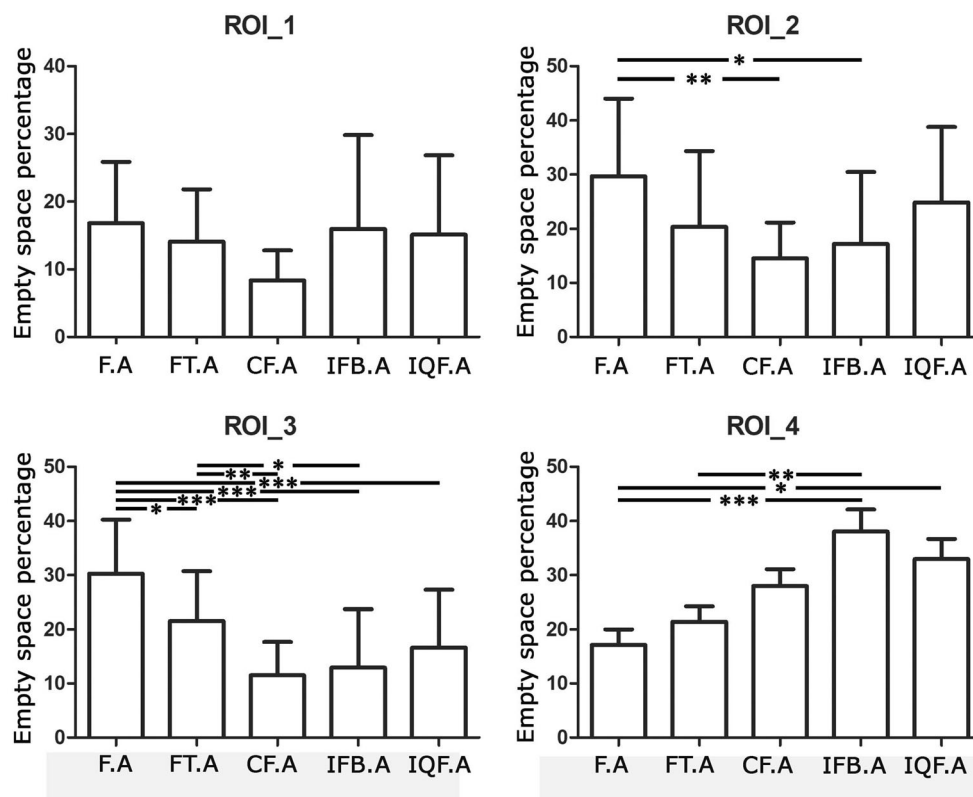
revealed significant differences in the percentages for ROI 2 ($F = 4.427$, $p < 0.01$), ROI 3 ($F = 12.98$, $p < 0.01$), and ROI 4 ($F = 6.368$, $p < 0.01$). The significance of the differences between the groups compared in pairs was further confirmed through the application of the subsequent Bonferroni test (Fig. 6). In summary, in ROI 1, there were no significant differences between the percentages of blank measured in F.A and each of the frozen categories in the study ($p > 0.05$); in ROI 2, a significantly different percentage was only highlighted between F.A and CF.A ($p < 0.05$) and F.A and IFB.A ($P < 0.01$) categories; in ROI 3, F.A category was significantly different from all the frozen categories ($p < 0.001$) and FT.A category only from CF.A ($p < 0.01$) and IFB.A ($p < 0.05$); finally, in ROI 4, significant differences were highlighted between F.A category and IFB.A ($p < 0.001$), and F.A and IQF.A ($p < 0.05$) (Fig. 6).

Parameters Finally Selected and Threshold Definition for Discriminating Fresh and Frozen Products

Mantle Parameters

Parameters a, b, c, and d achieved statistical significance in group comparisons (Table 3), confirming a relevant effect of freezing in the appearance of overall tissue structural alterations primarily represented by gapping and empty spaces or

Fig. 6 Graphical representation of the results of the empty space percentage within the axial nerve cord ROI in the various product categories included in the study. The significant differences found through the pair analysis of the data obtained for the individual categories are shown above each bar histogram (* $p < 0.05$; ** $p < 0.01$; *** $p < 0.001$)



lacunae between and within muscle bundles. These alterations are in accordance with those previously described in Indopacific squid (*Uroteuthis edulis*), Atlantic squid (*Illex argentinus*), and Indopacific cuttlefish (*Sepia pharaonis*) (Ueng and Chow 1998). Thus, the selected parameters were confirmed as objective histological indices for the discrimination of fresh and frozen common octopus. Empty space percentages and score indicative thresholds to discriminate fresh products were settled as follows: (1) a mean white space percentage of 25% corresponding to the upper confidence limit of F.M (95% CI = 20.95–24.98%); (2) a mean white space percentage between 25 and 33%, corresponding to the minimum white percentage measured in CF.M in association with the absence of optically empty spaces (score = 0) and absent or minimum muscle bundle gaping (score = 0) (Table 3). Contrariwise, mean white space percentages greater than 33% and the presence of empty spaces (score = 1) and gaping score = 1 or 2 were associated with frozen products.

Arm Parameters

Analogously, parameters b and c were confirmed as suitable indices of freezing process to be used for the analysis of tissue sections obtained from octopus' arm while two additional morphological parameters e and f (Table 4) were significant freezing process indices. On the contrary, the highlighting of optically empty spaces within the connective matrix surrounding the nerve, without any statistically significant difference between the different types of product under study (FA, FT.A, CF.A, IFB.A, IQF.A), led to the exclusion of parameter g from the indicators applicable for discriminatory purposes. Finally, according to the lack of significant differences highlighted in all the ROI defined within the axial nerve cord, the only identified morphometric parameter (parameter h) was definitively excluded from the indices applicable for discriminatory purposes.

Conclusion

The indication on seafood labeling of the preserving method used for processing is an essential and mandatory element in accordance with current EU legislation. Therefore, the omission of this information represents a fraud to the detriment of the interests and potentially of the health of the consumer, in relation to the commercial value and limited shelf life of thawed products. In the present study, after excluding morphological alterations evident during the shelf life of the fresh product maintained at 0 °C, the overall structural organization (a, e), the muscle bundle gaping (b), and the presence of optically empty spaces (c, f) were finally verified as suitable morphological parameters for the discrimination of fresh and thawed mantle and arms of common octopus, one of the

cephalopods most appreciated by Italian consumers. Moreover, between the morphometric parameters proposed, only the mean white space percentage between and within mantle muscles bundles (parameter d) showed significant differences between fresh and frozen/thawed octopus and may constitute a complementary parameter to be used in association with the aforesaid morphological parameters. Starting from the results of this study, an objective assessment grid could be settled and validated. It could be therefore used as an analytical tool both during the official and self-control checks for monitoring and preventing frauds at each stage of the value chain.

Acknowledgment The authors wish to thank the quality office of UNICOOP Firenze for its contribution to the research activities and sample collection.

Funding Information Open access funding provided by Università di Pisa within the CRUI-CARE Agreement. The study was performed with funds granted by the University of Pisa (Project PRA_2017_24).

Compliance with Ethical Standards

Conflict of Interests Tinacci Lara, Armani Andrea, Scardino Giulia, Guidi Alessandra, Nucera Daniele, Miragliotta Vincenzo, and Abramo Francesca declare that they have no conflict of interest.

Ethical Approval This article does not contain any studies with human or animal subjects. In particular, the cephalopods included in the study were already slaughtered and sold on the market for human consumption.

Informed Consent Informed consent is not applicable to this study.

Open Access This article is licensed under a Creative Commons Attribution 4.0 International License, which permits use, sharing, adaptation, distribution and reproduction in any medium or format, as long as you give appropriate credit to the original author(s) and the source, provide a link to the Creative Commons licence, and indicate if changes were made. The images or other third party material in this article are included in the article's Creative Commons licence, unless indicated otherwise in a credit line to the material. If material is not included in the article's Creative Commons licence and your intended use is not permitted by statutory regulation or exceeds the permitted use, you will need to obtain permission directly from the copyright holder. To view a copy of this licence, visit <http://creativecommons.org/licenses/by/4.0/>.

References

- Altissimi S, Mercuri ML, Framboas M, Tommasino M, Pelli S, Benedetti F, Bella SD, Haouet N (2017) Indicators of protein spoilage in fresh and defrosted crustaceans and cephalopods stored in domestic condition. *Ital J Food Saf* 6(4):6921. <https://doi.org/10.4081/ijfs.2017.6921>
- Ando M, Takenaga E, Hamase S, Yamane A (2005) Effect of super-chilling storage on maintenance of quality and freshness of swordtip squid *Loligo edulis*. *Food Sci Technol Res* 11(3):355–336. <https://doi.org/10.3136/fstr.11.3551>

- Arkhipkin AI, Rodhouse PGK, Pierce GJ, Sauer W, Sakai M, Allcock L, Arguelles J, Bower JR, Castillo G, Ceriola L, Chen CS, Chen X, Diaz-Santana M, Downey N, González AF, Granados Amores J, Green CP, Guerra A, Hendrickson LC, Ibáñez C, Ito K, Jereb P, Kato Y, Katugin ON, Kawano M, Kidokoro H, Kulik VV, Laptikhovskiy VV, Lipinski MR, Liu B, Mariátegui L, Marin W, Medina A, Miki K, Miyahara K, Moltschanivskiy N, Moustahfid H, Nabhitabhata J, Nanjo N, Nigmatullin CM, Ohtani T, Pecl G, Perez JAA, Piatkowski U, Saikiang P, Salinas-Zavala CA, Steer M, Tian Y, Ueta Y, Vijai D, Wakabayashi T, Yamaguchi T, Yamashiro C, Yamashita N, Zeidberg LD (2015) World squid fisheries. *Rev Fish Sci Aquac* 23(2):92–252. <https://doi.org/10.1080/23308249.2015.1026226>
- Armani A, D'Amico P, Cianti L, Pistolesi M, Susini F, Castigliero L, Guarducci M, Gianfaldoni D, Guidi A (2017) Assessment of food business operator training on parasitological risk management in sushi restaurants: a local survey in Florence, Italy. *J Environ Health* 80(2):1–8
- Bahuaud D, Mørkøre T, Langsrud Ø, Sinnes K, Veiseth E, Ofstad R, Thomassen MS (2008) Effects of -1.5 C super-chilling on quality of Atlantic salmon (*Salmo salar*) pre-rigor fillets: cathepsin activity, muscle histology, texture and liquid leakage. *Food Chem* 111(2): 329–339. <https://doi.org/10.1016/j.foodchem.2008.03.075>
- Barbosa A, Vaz-Pires P (2004) Quality index method (QIM): development of a sensorial scheme for common octopus. *Food Control* 15: 161–168. [https://doi.org/10.1016/S0956-7135\(03\)00027-6](https://doi.org/10.1016/S0956-7135(03)00027-6)
- Bartol IK (2001) Role of aerobic and anaerobic circular mantle muscle fibers in swimming squid: electromyography. *Biol Bull* 200:59–66. <https://doi.org/10.2307/1543085>
- Bone Q, Brown ER, Usher M (1995) The structure and physiology of cephalopod muscle fibers. In: Abbott NJ, Williamson R, Maddock L (eds) *Cephalopod neurobiology*. Oxford University Press, New York, pp 301–329
- Bozzetta E, Pezzolato M, Cencetti E, Varello K, Abramo F, Mutinelli F, Ingravalle F, Teneggi E (2012) Histology as a valid and reliable tool to differentiate fresh from frozen thawed fish. *J Food Prot* 75(8): 1536–1541. <https://doi.org/10.4315/0362-028X.JFP-12-035>
- Duflos G, Le Fur B, Mulak V, Becel P, Malle P (2002) Comparison of methods of differentiating between fresh and frozen-thawed fish or fillets. *J Sci Food Agric* 82:1341–1345. <https://doi.org/10.1002/jsfa.1195>
- EUMOFA (2018) The EU Fish market, 2018 edition. https://www.eumofa.eu/documents/20178/132648/EN_The+EU+fish+market+2018.pdf. Accessed 15 Jan 2020
- EUMOFA (2019) The EU Fish market, 2019 edition. https://www.eumofa.eu/documents/20178/157549/EN_The+EU+fish+market_2019.pdf. Accessed 15 Jan 2020
- FAO (2018) The State of World Fisheries and Aquaculture 2018—Meeting the Sustainable Development Goals. Rome. Licence: CC BY-NC-SA 3.0 IGO; <http://www.fao.org/3/i9540en/i9540en.pdf>. Accessed 15 Jan 2020
- FAO (2019) GLOBEFISH—Information and Analysis on World Fish Trade. <http://www.fao.org/in-action/globefish/market-reports/resource-detail/en/c/1199466/>. Accessed 15 Jan 2020
- FAO (2020) Species fact sheet, *Octopus vulgaris*. <http://www.fao.org/fishery/species/3571/en>. Accessed 24 Feb 2020
- Fossati S, Benfenati F, Zullo L (2011) Morphological characterization of the *Octopus vulgaris* arm. *Vie Milieu* 61(4):191–195
- George J, Van Wettere AJ, Michaels BB, Crain D, Lewbart GA (2016) Histopathologic evaluation of postmortem autolytic changes in bluegill (*Lepomis macrochirus*) and crappie (*Pomoxis anularis*) at varied time intervals and storage temperatures. *Peer J* 4:1943. <https://doi.org/10.7717/peerj.1943>
- Ghaly AE, Dave D, Budge S, Brooks MS (2010) Fish spoilage mechanisms and preservation techniques. *Am J Appl Sci* 7(7):859–877. <https://doi.org/10.3844/ajassp.2010.859.877>
- Gokoglu N, Yerlikaya P (2015) Thawing of the fish. In: Gokoglu N and Yerlikaya P (eds). *Seafood chilling, refrigeration and freezing: science and technology*. John Wiley & Sons, Ltd., The Atrium, Southern Gate, West Sussex, pp 208–227
- Gokoglu N, Topuz OK, Gokoglu M, Tokay FG (2017) Characterization of protein functionality and texture of tumbled squid, octopus and cuttlefish muscles. *J Food Meas Charact* 11(4):1699–1705. <https://doi.org/10.1007/s11694-017-9550-1>
- Gokoglu N, Topuz OK, Yerlikaya P, Yatmaz HA, Ucak I (2018) Effects of freezing and frozen storage on protein functionality and texture of some cephalopod muscles. *J Aquat Food Prod Technol* 27(2):211–218. <https://doi.org/10.1080/10498850.2017.1422168>
- Graziadei P (1965) Muscle receptors in cephalopod. *P Roy Soc B-Bol Sci* 161:392–402. <https://doi.org/10.1098/rspb.1965.0011>
- Hurtado JL, Borderías J, Montero P, An H (1999) Characterization of proteolytic activity in octopus (*Octopus vulgaris*) arm muscle. *J Food Biochem* 23(4):469–483. <https://doi.org/10.1111/j.1745-4514.1999.tb00031.x>
- Hurtado JL, Montero P, Borderías J (2001) Chilled storage of pressurized octopus (*Octopus vulgaris*) muscle. *J Food Sci* 66(3):400–406. <https://doi.org/10.1111/j.1365-2621.2001.tb16117.x>
- ISMEA, (2019) mercati, pesca & acquacoltura. <http://www.ismea.it/flex/cm/pages/ServeBLOB.php/L/IT/IDPagina/1488>. Accessed 15 December 2019
- Katsanidis E (2004) Impact of physical and chemical pretreatments on texture of octopus (*Eledone moschata*). *J Food Sci* 69(7):264–267. <https://doi.org/10.1111/j.1365-2621.2004.tb13626.x>
- Khan BM, Liu Y (2019) Marine mollusks: food with benefits. *Compr Rev Food Sci Food Saf* 18(2):548–564. <https://doi.org/10.1111/1541-4337.12429>
- Kiani H, Sun DW (2011) Water crystallization and its importance to freezing of foods: a review. *Trends Food Sci Technol* 22(8):407–426. <https://doi.org/10.1016/j.tifs.2011.04.011>
- Kier WM (2016) The musculature of coleoid cephalopod arms and tentacles. *Front Cell Dev Biol* 4:10. <https://doi.org/10.3389/fcell>
- Kier WM, Stella MP (2007) The arrangement and function of octopus arm musculature and connective tissue. *J Morphol* 268(10):831–843. <https://doi.org/10.1002/jmor.10548>
- Kier WM, Thompson JT (2003) Muscle arrangement, function and specialization in recent coleoids. *Berliner Paläobiologische Abhandlungen* 3:141–162. https://www.geo.fu-berlin.de/geol/fachrichtungen/pal/ressourcen/berliner-palaeobiologische-abhandlungen/Band_03/14.pdf. Accessed 21 February 2020
- Kolbe E, Kramer D (2007) Planning for seafood freezing. Alaska Sea Grant College Program. Cooper Publishing, Alaska, pp. 112
- Lavety J (1991) Physio-chemical problems associated with fish freezing. In Bald WB (ed) *Food freezing: today and tomorrow*. Springer Series in Applied Biology. Springer-Verlag, London. pp. 123–131
- Leistner L (2000) Basic aspects of food preservation by hurdle technology. *Int J Food Microbiol* 55:181–186. [https://doi.org/10.1016/S0168-1605\(00\)00161-6](https://doi.org/10.1016/S0168-1605(00)00161-6)
- Lougovois VP, Kolovou MK, Savva IN, Kontominas MG (2008) Spoilage potential of ice-stored whole musky octopus (*Eledone moschata*). *Int J Food Sci Technol* 43(7):1286–1294. <https://doi.org/10.1111/j.1365-2621.2007.01607.x>
- Love RM, Robertson I (1968) The connective tissues of fish: I. The influence of biological condition in cod on gaping in frozen-thawed muscle. *Int J Food Sci Technol* 3(3):215–221. <https://doi.org/10.1111/j.1365-2621.1968.tb01459.x>
- Love RM, Lavety J, Steel PJ (1969) The connective tissues of fish II. Gaping in commercial species of frozen fish in relation to rigor mortis. *Int J Food Sci Technol* 4(1):39–44. <https://doi.org/10.1111/j.1365-2621.1969.tb01495.x>
- Meistro S, Pezzolato M, Muscolino D, Giarratana F, Baioni E, Panebianco A, Bozzetta E (2016) Histology as a valid tool to

- differentiate fresh from frozen-thawed marinated fish. *J Food Prot* 79(8):1457–1459. <https://doi.org/10.4315/0362-028X.JFP-16-007>
- Mommsen TP, Ballantyne J, MacDonald D, Gosline J, Hochachka PW (1981) Analogues of red and white muscle in squid mantle. *P Natl Acad Sci USA* 78(5):3274–3278. <https://doi.org/10.1073/pnas.78.5.3274>
- Mouritsen OG, Styrbaek K (2018) Cephalopod gastronomy—a promise for the future. *Frontiers in Comm* 3:38. <https://doi.org/10.3389/fcomm.2018.00038>
- Pavlov A, Dimitrov D, Penchev G, Georgiev L (2008) Structural changes in common carp (*Cyprinus carpio* L.) fish meat during freezing. *Bulg J Vet Med* 11(2):131–136
- Petzold G, Aguilera JM (2009) Ice morphology: fundamentals and technological applications in foods. *Food Biophys* 4:378–396. <https://doi.org/10.1007/s11483-009-9136-5>
- Pham QT (2008) Advances in food freezing/thawing/freeze concentration modelling and techniques. *Japan J Food Eng* 9(1):21–32. <https://doi.org/10.11301/jsfe2000.9.21>
- Popelka P, Nagy J, Pipová M, Marcinčák S, Lenhardt L (2014) Comparison of chemical, microbiological and histological changes in fresh, frozen and double frozen rainbow trout (*Oncorhynchus mykiss*). *Acta Vet Brno* 83(2):157–161. <https://doi.org/10.2754/avb201483020157>
- Preuss T, Lebaric ZN, Gilly WF (1997) Post-hatching development of circular mantle muscles in the squid *Loligo opalescens*. *Biol Bull* 192(3):375–387. <https://doi.org/10.2307/1542747>
- Regulation (EU) No 1169/2011 (2011) of the European Parliament and of the Council of 25 October 2011 on the provision of food information to consumers, amending Regulations (EC) No 1924/2006 and (EC) No 1925/2006 of the European Parliament and of the Council, and repealing Commission Directive 87/250/EEC, Council Directive 90/496/EEC, Commission Directive 1999/10/EC, Directive 2000/13/EC of the European Parliament and of the Council, Commission Directives 2002/67/EC and 2008/5/EC and Commission Regulation (EC) No 608/2004 OJ L 304, 22.11.2011:18–63
- Regulation (EU) No 1379/2013 (2013) of the European Parliament and of the Council of 11 December 2013 on the common organisation of the markets in fishery and aquaculture products, amending Council Regulations (EC) No 1184/2006 and (EC) No 1224/2009 and repealing Council Regulation (EC) No 104/2000. OJ L 354, 28.12.2013:1–21
- Roy BC, Ando M, Itoh T, Tsukamasa Y (2012) Structural and ultrastructural changes of full-cycle cultured Pacific bluefin tuna (*Thunnus orientalis*) muscle slices during chilled storage. *J Dermatol Sci* 92(8):1755–1764. <https://doi.org/10.1002/jsfa.5542>
- Shalini R, Shakila RJ, Jeyasekaran G, Jeevithan E (2015) Sensory, biochemical and bacteriological properties of octopus (*Cistopus indicus*) stored in ice. *J Food Sci Technol* 52(10):6763–6769. <https://doi.org/10.1007/s13197-015-1751-1>
- Sharifian S, Alizadeh E, Mortazavi MS, Moghadam MS (2014) Effects of refrigerated storage on the microstructure and quality of grouper (*Epinephelus coioides*) fillets. *J Food Sci Technol* 51(5):929–935. <https://doi.org/10.1007/s13197-011-0589-4>
- Shigemura Y, Ando M, Tsukamasa Y, Makinodan Y, Kawai T (2003) Correlation of type V collagen content with post-mortem softening of fish meat during chilled storage. *Fish Sci* 69(4):842–848. <https://doi.org/10.1046/j.1444-2906.2003.00696.x>
- Strateva M, Penchev G (2019) Histological discrimination of fresh from frozen/thawed carp (*Cyprinus carpio*). *Bulg J Vet Med* 1:1–8. <https://doi.org/10.15547/bjvm.2019-0113>
- Sykes AV, Oliveira AR, Domingues PM, Cardoso CM, Andrade JP, Nunes ML (2009) Assessment of European cuttlefish (*Sepia officinalis*, L.) nutritional value and freshness under ice storage using a developed quality index method (QIM) and biochemical methods. *LWT Food Sci Technol* 42(1):424–432. <https://doi.org/10.1016/j.lwt.2008.05.010>
- Tinacci L, Ammani A, Guidi A, Nucera D, Shvartzman D, Miragliotta V, Coli A, Giannesi E, Stornelli MR, Fronte B, Di Iacovo F, Abramo F (2018) Histological discrimination of fresh and frozen/thawed fish meat: European hake (*Merluccius merluccius*) as a possible model for white meat fish species. *Food Control* 92:154–161. <https://doi.org/10.1016/j.foodcont.2018.04.056>
- Uddin M (2010) Differentiation of fresh and frozen-thawed fish. In Nolle LML, Toldra F (Eds.), *Handbook of seafood and seafood products analysis*. CRC Press, Taylor and Francis ebooks. pp. 735–750
- Ueng YE, Chow CJ (1998) Textural and histological changes of different squid mantle muscle during frozen storage. *J Agric Food Chem* 46(11):4728–4733. <https://doi.org/10.1021/jf9803278>
- Upton HF (2015) Seafood fraud. *Congressional Research Service*. April 7, 2015, www.crs.gov, RL34124, <http://nationalaglawcenter.org/wp-content/uploads/assets/crs/RL34124.pdf>. Accessed 21 February 2020
- Vaz-Pires P, Barbosa A (2004) Sensory, microbiological, physical and nutritional properties of iced whole common octopus (*Octopus vulgaris*). *LWT Food Sci Technol* 37(1):105–114. [https://doi.org/10.1016/S0023-6438\(03\)00141-5](https://doi.org/10.1016/S0023-6438(03)00141-5)
- Vaz-Pires P, Seixas P (2006) Development of new quality index method (QIM) schemes for cuttlefish (*Sepia officinalis*) and broadtail shortfin squid (*Illex coindetii*). *Food Control* 17(12):942–949. <https://doi.org/10.1016/j.foodcont.2005.07.004>
- Venugopal V (2006). Quick freezing and individually quick frozen products. In: Venugopal (Ed.), *Seafood processing*. Taylor and Francis, CRC Press, New York. pp. 95–140
- Vieites JM, Ruiz CS, Fernández F, Alonso RC (2019) Importance of cephalopod health and welfare for the commercial sector. In: Gestal C, Pascual S, Guerra A, Fiorito G, Vieites JM (eds) *Handbook of pathogens and diseases in cephalopods*. Springer Nature, Switzerland, AG, Open access. pp. 5–7

Publisher's Note Springer Nature remains neutral with regard to jurisdictional claims in published maps and institutional affiliations.